EXPERIMENTAL INVESTIGATION OF A NOVEL FRP-CONCRETE COMPOSITE FLOOR SLAB

Xian Gai, Antony Darby, Tim Ibell and Mark Evernden
BRE Centre for Innovative Construction Materials,
Department of Architecture and Civil Engineering, University of Bath,
Bath BA2 7AY, United Kingdom

ABSTRACT

This paper presents the findings of an experimental investigation of a novel FRP-concrete composite floor system. The system consists of a moulded glass fibre reinforced polymer (GFRP) grating adhesively bonded to square pultruded GFRP box sections as structural formwork for a concrete slab. Holes cut into the top flange of the box sections at a variable spacing allow concrete 'studs' to form at the grating/box section interface. During casting, GFRP dowels are inserted into the holes to further connect the grating and box sections. Following component tests on the concrete-filled grating and shear connectors, six (300 x 150) mm and 3000 mm long slab specimens were designed and tested under five-point bending. From the resulting load-deflection curves, it was determined that all specimens behaved elastically and fully compositely until the initial peak was reached. No slip was observed between the concrete and GFRP box sections until the longitudinal shear failure occurred at the initial peak. The load capacity carried on increasing at a reduced stiffness in a progressive manner, with significant residual strength and slip observed. All specimens failed by the separation of the webs and flange at the upper corners of the box sections due to the large curvature induced. Full-scale experimental results demonstrated that the controlled longitudinal shear failure provided deformability to the overall system and a robust interaction between the concrete and FRP formwork was achieved.

INTRODUCTION

Conventional reinforced concrete structures are fabricated by casting concrete in temporary formworks that are usually made from timber or steel. The formworks are often held in place by temporary scaffolding. Upon hardening of the concrete, the formworks and temporary support are removed, revealing the concrete structure within. Permanent participating formwork, also referred to as a stay-in-place (SIP) system, remains structurally integrated with the concrete and provides structural strength to the overall system. It not only acts as a self-supporting formwork during construction, but also acts as an external, durable, structural reinforcement.

The elimination of conventional reinforcing bars can significantly simplify the engineering and detailing process, as well as saving time during construction. In the past few decades Fibre Reinforced Polymers (FRPs) composite materials have been widely used as an alternative solution to the conventional steel reinforcement in new-build structures and as

the external reinforcements for the retrofitting and strengthening of existing structures. These materials have numerous potential advantages over the traditional materials particularly in terms of strength-to-weight ratio and durability. Within the new build sector, there has been a significant interest in the use of FRP-concrete hybrid system in concrete decks and slabs. A number of hybrid systems have been developed, where FRP materials were used as a structurally integrated stay-in-place formwork for concrete. The system has the benefit of simplifying the construction process related to the speed and ease of construction.

Fam et al. [1] developed and tested rectangular concrete-filled filament-wound GFRP tubes in flexure. Later, Fam and Skutezky [2] added a thin concrete layer on the top of the concrete-filled pultruded rectangular GFRP tubes, with the two parts mechanically bonded using GFRP dowels embedded into the tubes. They also studied the effects of concrete filling of the tubes, length of shear span, and CFRP lamination of the GFRP tension flange. The experiments demonstrated that the dowels used in the concrete-filled GFRP tube-slab system provide better slip resistance and composite action than those used in the hollow GFRP tube-slab system, and that the concrete filling has a substantial effect on initial stiffness but a small effect on strength. However, the failure mode subsequently changes from a shear failure of the GFRP dowels to sudden rupture of the GFRP tension flange, which has no ductility at all.

In this paper, the concept of concrete-filled GFRP box beams is taken a step further, by adding a concrete-filled GFRP moulded grating acting compositely with two GFRP box sections, as shown in Fig. 1(a) and (b). The proposed FRP-concrete composite floor slab consists of two layers of different materials: pultruded hollow GFRP box section to resist the tensile forces and moulded GFRP grating filled with concrete to resist the compressive forces. FRP materials are inherently non-ductile, so other means of providing progressive failure of the system are required. Thus, to provide ductility, the concrete in compression is utilised. The unconfined concrete has minimal ductility. However, by utilizing an FRP moulded grating filled with concrete in the compression zone, the concrete is confined, allowing much greater strain capacity to be developed which increases the overall ductility. The requirement of providing a robust connection between the GFRP box section in tension and the concrete in compression is addressed by using GFRP dowels combined with concrete studs formed along the grating/box section interface as shown in Fig. 1(c). During concrete casting, foam block was inserted into the box sections in order to remove unnecessary concrete in tension zone and hold the dowels in place. GFRP dowels were then pushed into foam block through these holes which were cut on the surface of the box sections.

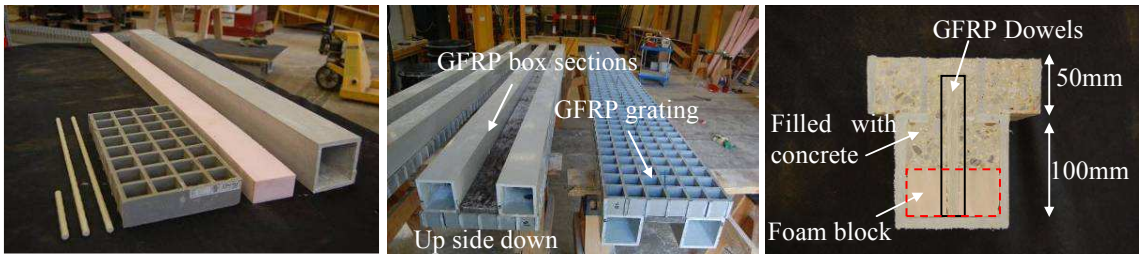

(a) (b) (c)

Figure 1. The key sectional materials, the proposed FRP formwork and shear connection

Push-out tests were used to assess the robustness of the proposed shear connectors and to study their load-slip behaviour. Fig. 2 shows the push-out tests set-up and load-slip plot of shear connectors. Two push-out specimens were tested to compare the load-slip responses of four GFRP dowels with eight GFRP dowels embedded in a partially concrete-filled GFRP box section. The test specimens were fabricated by bonding two identical units back to back. The shear connection between the grating and box sections was shown in Fig. 1(c). The schematic test arrangement for investigating the load-slip behaviour of the proposed shear connectors is presented in Fig. 2. As shown in the load-slip plot in Fig. 2, both specimens had an extremely high initial stiffness provided by the adhesive at the FRP/FRP interface and the concrete studs at the concrete/FRP interface. After the initial peak, the applied shear was then resisted by friction between the crack faces and by dowel action of the GFRP dowels crossing the crack, as shown in Fig. 3. Therefore, the residual strength, represented by a plastic plateau, was provided by the GFRP dowels acting in tension and shear along the shear crack interface and a progressive failure mechanism can be achieved. More details of push-out tests are discussed in Gai et al. [3]. Push-out test results demonstrate the potential for achieving both ductility and a robust interaction between the FRP formwork and the concrete. Experiments on full-scale slab tests are presented below to examine whether the ductility provided by the longitudinal shear failure can be achieved in the prototype system. This composite system is mainly designed as a one-way spanning floor system for building construction.

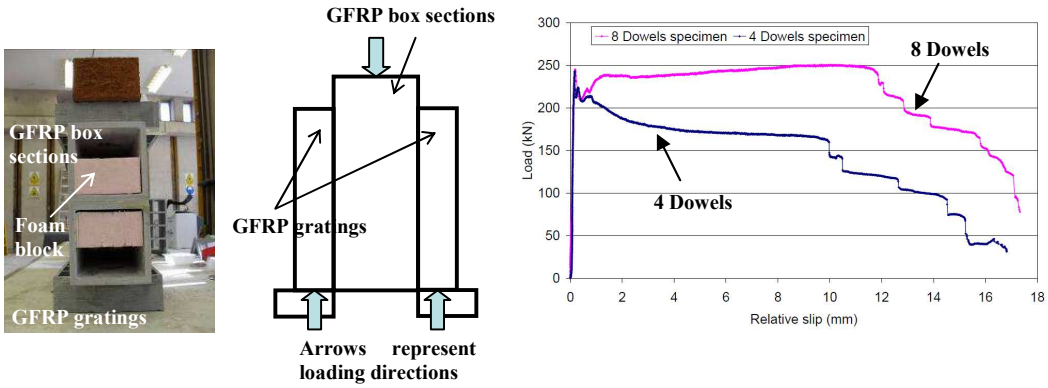

Figure 2. Push-out test specimens, tests setup and load-slip plot of shear connectors

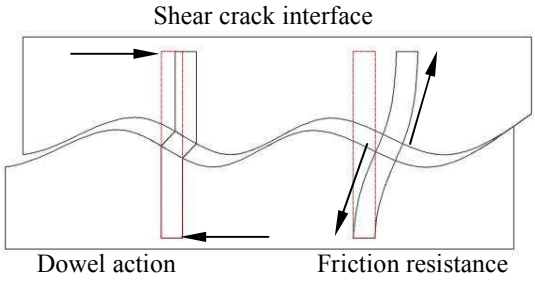

Figure 3. GFRP dowels acting in tension and shear along the crack interface

EXPERIMENTAL PROGRAM

This study aims at experimentally examining the failure behaviour of composite FRP-concrete hybrid slabs in order to verify whether its corresponding failure mode (longitudinal shear failure at the grating/box section interface) can provide sufficient ductility to the overall system. The experimental program included the testing of the proposed FRP-concrete composite slab to study its performance and ductility. Based on the findings of component tests, six slab tests were designed and tested under five-point bending.

Material Properties

In this study, pultruded GFRP box sections, GFRP dowels, foam blocks, moulded GFRP grating and concrete were used as shown in Fig. 1. The following sections provide a detailed description of the different materials.

Commercially available GFRP pultruded box sections (100x100x8) mm supplied by Fibreline Composites, Denmark, were used as the tension component. The longitudinal roving and multidirectional mats provide longitudinal and transverse strength and stiffness. The box section had a longitudinal tensile strength of 240 MPa and elastic modulus of 23 GPa, as specificed by the manufacturer tested according to European Standard EN 13706 (Fibreline Composites Design Manual, Fibreline Composites Ltd).

Aslan 100 GFRP pultruded rebar of 10mm diameter, composed of E-glass fibres of minimum 70% fibre content by weight and vinylester resin, were supplied by Hughes Brothers and were used as dowels in this study. The sand coated bars had a longitudinal tensile strength, elastic modulus and shear strength of 760 MPa, 40.8 GPa and 152 MPa respectively (Aslan 100 GFRP rebar Data Sheet, Hughes Brothers Ltd).

Commercially available panels of moulded GFRP grating (50x50 mm grid size) were cut into (300x3000) mm strips for fabrication of the slab specimens. The bi-directional grating, which was 50 mm thick with a 35-40 % fibre volume fraction, had a tensile strength and elastic modulus of 172 MPa and 15 GPa respectively in both longitudinal and transverse directions (Fibreline Composites Design Manual, Fibreline Composites Ltd).

The concrete compressive strength ranged from 26 MPa to 31 MPa with an average of 29 MPa based on cube tests. Super-plasticizer was used in order to make the concrete more workable and self-flowing, allowing the concrete to easily fill the small holes without excessive compaction.

Details of Full-scale Slab Test Specimens

The prototype slab specimens are composed of two 3 m long GFRP box sections (100x100x8) mm adhesively bonded to 300 mm wide, 3 m long moulded GFRP grating using two-component epoxy adhesive Araldite 2015. Both components are connected at a variable spacing using 88 mm long sand-coated GFRP dowels (diameter 10 mm) embedded into the concrete. 38 mm diameter holes are drilled on the top flange of the box sections in order to push the GFRP dowels into the 44 mm thick foam block and allow the concrete to fill the remaining 40mm of the box section. Once the concrete is cured, the top half of GFRP dowels were anchored in the concrete filled lattice of the grating, since the grating was completely filled with concrete. The bottom half of dowels were embedded in the partially concrete filled GFRP box sections (40mm deep embedment in concrete). The composite action between the grating and box sections during the concrete casting initially relies on the adhesive bond. After settlement of the concrete, the GFRP dowels and concrete studs formed around these 38 mm holes act compositely to resist longitudinal shear at the grating-box sections interface. The cross section of the slab specimen is shown in Fig. 4. Red dash lines in Fig. 4 represent the regions filled by the concrete.

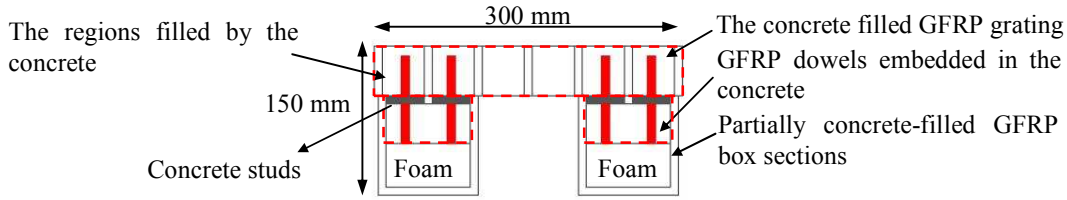

Figure 4. The cross section of the slab specimen

The objective of the slab tests is to verify the concept of utilizing the post-yielding characteristics of the proposed shear connector, as shown in Fig. 2, to provide ductility to the overall system. Six slab specimens were prepared in two groups. The first group contained specimens S_1, S_2 and S_3, and the second group contained specimens S_4, S_5, S_6. The first group of specimens were designed with different spacing of shear connectors used at the concrete/FRP interface to obtain the optimum number of shear connectors, giving better post-yielding characteristics. As specimen S_3 exhibited a ductile behaviour similar to specimens S_1 and S_2, specimens S_4 and S_6 were designed to have an identical number of shear connectors as specimen S_3. The reason for choosing the design of specimen S_3 is because the ultimate load capacity (80 kN) in specimen S_3 is the closest to the service load capacity (20 kN calculated from the service loading deflection limit – span/300), meaning more efficient use of materials. Specimens S_4 and S_6 were tested using different loading schemes. Specimen S_5 was designed to have an identical number of GFRP dowels to specimen S_3 with higher number of holes to improve concrete flow. A schematic drawing of the dowel position of each specimen is shown in Fig. 5.

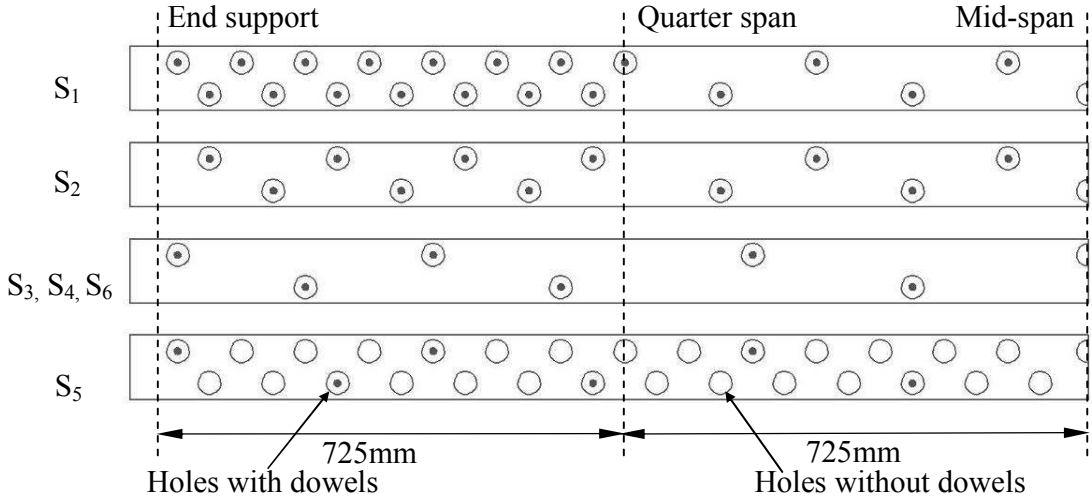

Figure 5. Distribution of holes with and without dowels in specimens S_1-S_6

Test Set-up and Instrumentations

Each specimen was tested using a five-point bending setup with a span of 2900 mm, and 725 mm between each loading point. The end support conditions are one roller support and one pin support. Linear variable differential transducers were used to monitor mid-span deflections, as well as the relative end slip between the concrete filled grating and the GFRP box sections. Although buildings are generally designed using uniformly distributed loads, it is not necessarily the worst case in reality and point loads should also be considered. Therefore, the point load envelope was chosen to simulate the worst case scenario in building construction. There are two types of loading schemes – Type A and Type B. A schematic drawing of both setups is shown in Fig. 6.

Type A Loading

Specimen S_1 was tested with three equal point loads with a load increment of 2 kN (referred to as Type A). This loading configuration is to simulate the bending moment envelope, which is caused by a single point load moving along the span from one support to the other. Specimen S_6 was also tested under Type A loading.

Type B Loading

Specimens S_2 and S_3 were tested with three point loads, however, the mid-span loading was twice as much as the loading on each of the quarter spans (referred to as Type B). Thus, the load was applied at a load increment of 2 kN in the two jacks located in each of the quarter span, and at a load increment of 4 kN in the mid-span jack. This loading configuration is to simulate the shear force envelope caused by a single point load moving along the span from one support to the other. Specimens S_4 and S_5 were also tested under Type B loading.

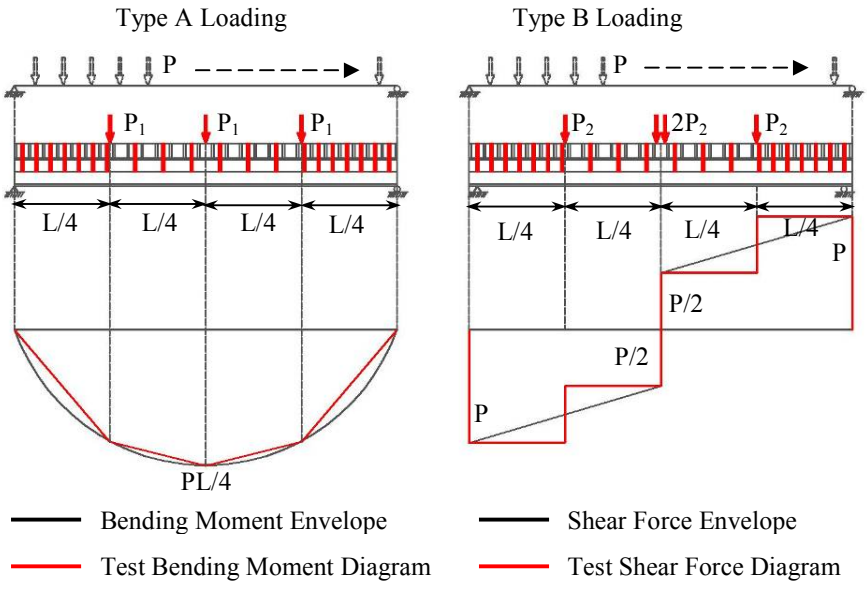

Figure 6. Type A loading and Type B loading schemes

EXPERIMENT RESULTS AND DISCUSSIONS

The load-deflection plot for specimens S_1-S_3 is shown in Fig. 7. The initial response of all the slab specimens was elastic, producing a stable, relatively linear relationship between the load and the deflection. This linear relationship indicated fully composite behaviour prior to the initial peak load. It is evident from Fig. 7, prior to the initial peak load, the stiffness of specimens S_1-S_3 are quite similar. This is logical because all specimens have the same cross-sectional configurations, therefore behaved similarly.

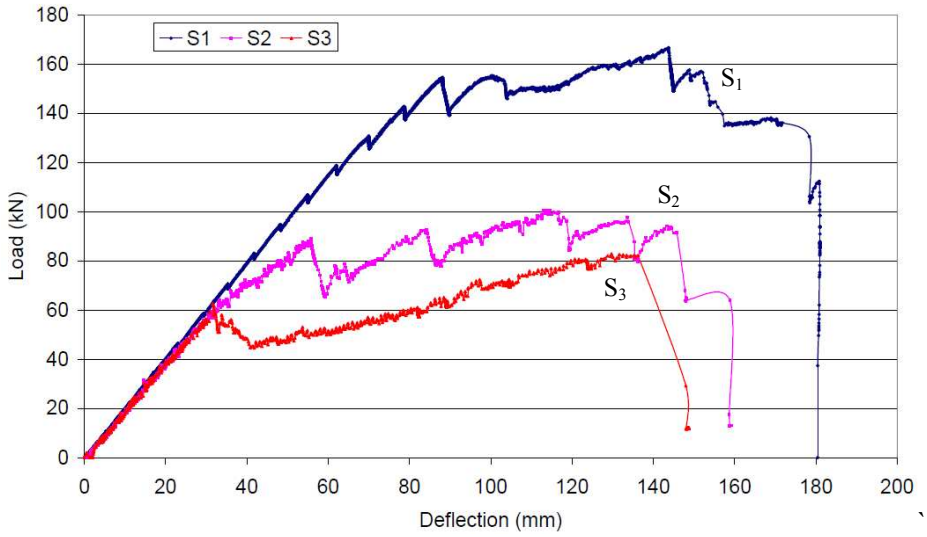

Figure 7. Load-deflection plot of specimens S_1, S_2 and S_3

As shown in Fig. 8, none of the three specimens exhibited any horizontal slip at the grating/box sections interface prior to reaching the initial peak load, indicating that all specimens behaved monolithically. It is to be noted that the initial peak load is determined by the adhesion between the concrete/FRP interface and the glued FRP-FRP interface. Thus, even though the adhesive FRP-FRP bond (referred to as mechanism M_1) is the same for all three specimens, the mechanical bond at the concrete/FRP interface through GFRP dowels (referred to as mechanism M_2) combined with the concrete studs (referred to as mechanism M_3) was reduced from specimens S_1 to S_3. This explained why specimen S_1 achieved the highest initial peak load, followed by specimens S_2 and S_3. Beyond this initial peak load, all three specimens exhibited a slight drop in load capacity, followed by a rebound to the initial peak and all carried on increasing load but at a reduced stiffness until they reached the final failure. This was likely to have been caused by a failure of its M_1 and M_3 bond mechanisms first (failure of glue and cracking of concrete), leaving only mechanism M_2 (GFRP dowels) responsible for resisting longitudinal shear at the concrete/FRP interface. It is logical that mechanism M_2 alone would result in a reduced stiffness because it solely depends upon shear and tensile resistance of GFRP dowels. After the initial peak load, as evident from Fig. 8, the relative end slip at the grating/box sections interface on the roller support side of specimens significantly increased, indicating that the composite action was compromised.

Eventually, the test specimens showed a sudden, dramatic loss of stiffness which ended the tests. This sudden loss of stiffness was the result of the local buckling of the pultruded box section directly under the loading head. This local loss of stiffness consequently changed the deflected shape, and introduced sharp curvatures in the central-span underneath the loading head. Separation of the webs and flange at the upper corners of the cross-sections has occurred as shown in Fig. 9. Local fibre breakage and delamination in the webs of the box sections were apparent from Fig. 9. This damage appeared simultaneously with the separation of the webs and flange at the upper corners of the cross-section, and was present in both webs of the box section. The damage was a result of the local buckling of both webs. The lateral deflection introduced local bending curvatures, and was facilitated by the separation of the webs from the top flange.

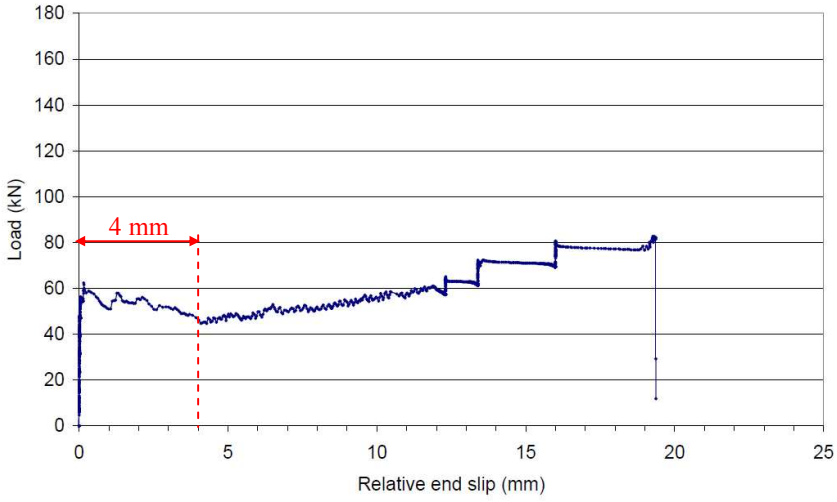

Figure 8. Load-relative end slip plot of specimen S_3

Figure 9. Web-flange separation failure and fibre breakage

After the tests of specimens S_1-S_3, three specimens S_4-S_6 were designed and tested to validate the test data by following the design of S_3. Specimens S_3 and S_4 were designed to have an identical number of shear connectors and both tested in Type B loading. Therefore both test results are directly comparable as shown in Fig. 10.

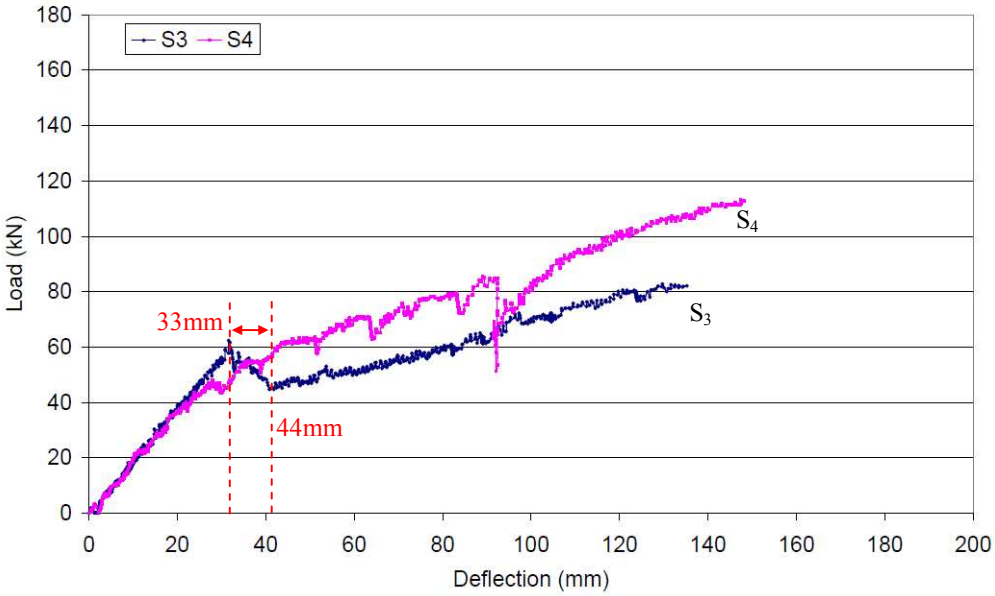

Figure 10. Load-deflection plot of specimens S_3 and S_4

Fig. 10 shows the initial stiffness of specimens S_3 and S_4 were identical. The initial peak load of specimen S_4 was slightly lower compared with that of specimen S_3, this might be due to the fact that the concrete strength in specimen S_4 was lower than that in specimen S_3, causing a reduction in contribution of mechanism M_3 (concrete studs). It also can be seen from Fig. 10 that there was a sudden drop in load capacity immediately after the initial peak in specimen S_3, however specimen S_4 exhibited a gradual reduction in stiffness without any drop in load capacity. The drop in load capacity in specimen S_3 might be caused by a sudden increase of slip after the initial peak, as shown in Fig. 8. The relative end slip dramatically increased from no visible slip at the initial peak (the corresponding deflection is 33 mm) to 4 mm slip at the lowest point (the corresponding deflection is 44 mm). However, the slip between the same deflection period in specimen S_4 was only 1 mm, as

shown in Fig. 11. The increase in the slip in specimen S_3 might be caused by the fact that there were large air voids in the concrete-fill inside the box sections in the central region, and as a result some of the dowels did not contribute to resisting the longitudinal shear. Therefore, the dowel action was not fully mobilised at this region, causing a reduction in longitudinal shear resistance and a significant increase in slip. This explained why specimen S_3 exhibited a drop in load capacity after the initial peak. Furthermore, the ultimate failure load in specimen S_3 (82 kN) was also lower than that of specimen S_4 (112 kN), this was also caused by the fact some of the dowels in specimen S_3 did not resist the shear due to voids in the concrete-fill in the box sections.

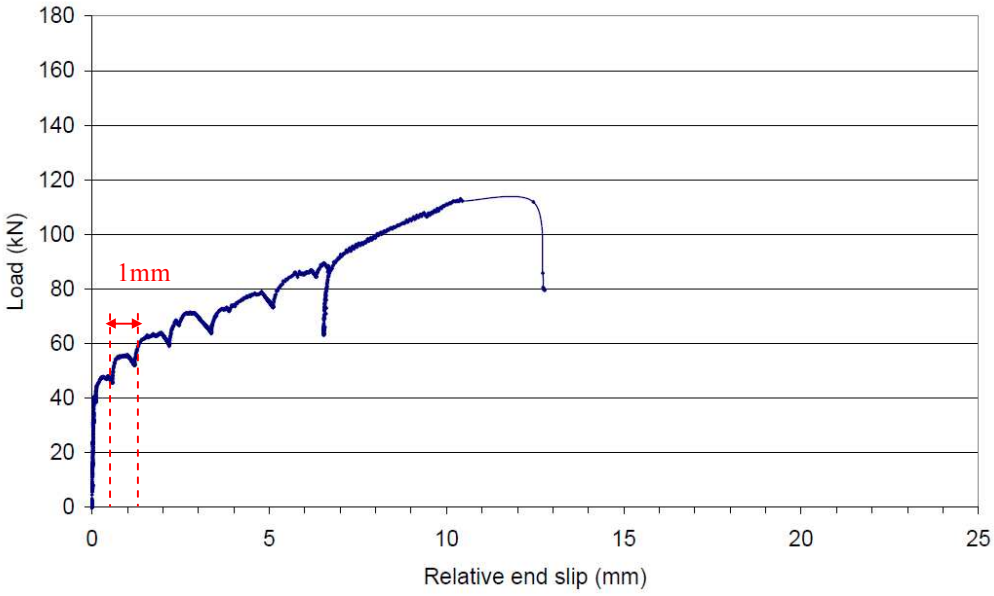

Figure 11. Load-relative end slip plot of specimen S_4

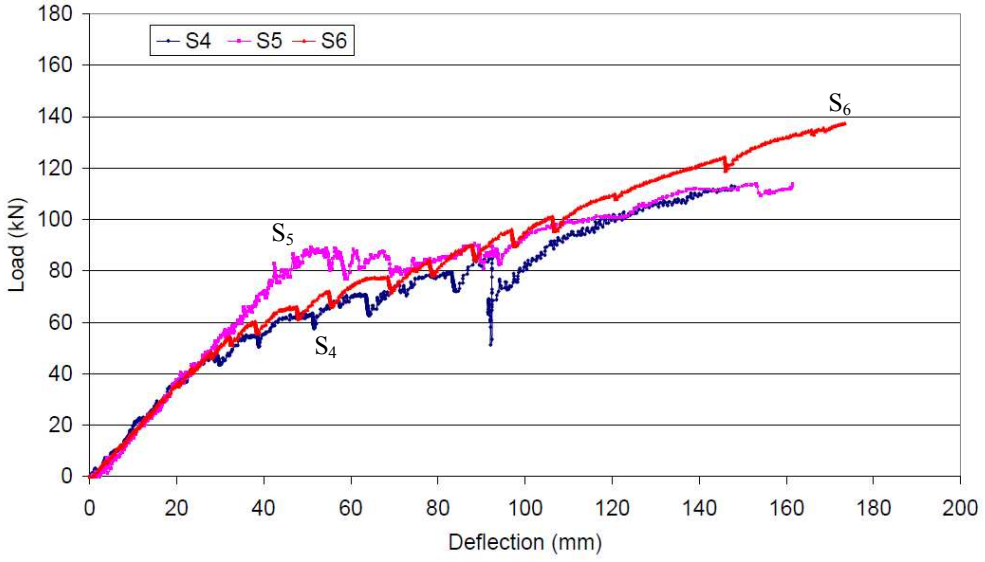

Figure 12. Load-deflection plot of specimens S_4, S_5 and S_6

The load-deflection plots for specimens S_4-S_6 were compared in Fig. 12. It was evident from this plot that, the stiffness of specimens S_4-S_6 were quite similar prior to the initial peak load. It is logical that specimen S_5 achieved the highest initial peak load, as the bond mechanism M_3 in specimen S_5 was enhanced by having additional concrete studs. After the initial peak, all specimens carried on increasing their load capacity at a relatively similar stiffness without a drop in load capacity until they reached the final failure, this is because only mechanism M_2 contributes to resisting the shear and the number of GFRP dowels are the same for specimens S_4-S_6, therefore the post initial peak behaviour of three specimens were similar.

CONCLUSIONS

1. All slab specimens behaved elastically and fully compositely until longitudinal shear failure occurred at the grating/box sections interface, after this the specimens carried on increasing load capacity at a reduced stiffness to the second peak until the final failure due to the web-flange separation. All specimens failed in a progressive manner, providing reasonable ductility to the overall system.

2. The comparison amongst specimens S_1-S_3 showed that the initial peak load, which is the end of elastic phase, is determined by the adhesion at the glued FRP/FRP interface (adhesive bond) and by the combination of friction and dowel action at the concrete/FRP interface (GFRP dowels combined with concrete studs).

3. The comparison amongst specimens S_4-S_6 showed that the post yielding behaviour is solely dependent on the shear resistance (Dowel action) and tensile resistance (Friction resistance) of GFRP dowels.

4. The design of specimen S_5 aimed to resolve the construction issue arising from the poor concrete filling by introducing more holes to improve concrete flow. It achieved a similar ductile failure behaviour compared with specimens S_4 and S_6. This also shows the flexibility of positioning the dowels, meaning the dowels can be altered to fit different loading requirements.

To conclude, the experimental results demonstrated that the proposed assembly provided ductility to the overall system in terms of energy absorption and a robust interaction between FRP formwork and concrete.

ONGOING AND FUTURE WORK

The analytical model for predicting the failure behaviour is divided into two parts – linear elastic analysis and ultimate capacity of the local web buckling prediction. The initial peak load can be reasonably predicted by assuming the fully composite action and a failure criterion in longitudinal shear failure, referred to as linear-elastic analysis. The shear flow resistance is calculated based on the load-slip characteristics of shear connectors, as previously shown in Fig. 2. Local web buckling prediction to predict the ultimate failure load is still ongoing. This prediction will be assessed at a later date against experimental

results, and comparisons between theory and experimental results presented at the conference.

ACKNOWLEDGEMENTS

The authors wish to acknowledge the support of Fiberline Composites, Denmark, supplier of the Moulded GFRP gratings and Pultruded GFRP box sections. The authors are also grateful to Brian Purnell, William Bazeley, and Neil Price at the University of Bath for their assistance during the experimental program. This research is funded by Building Research Establishment (BRE) Trust.

REFERENCES

1. Fam, A., Mandal, S., and Rizkalla, S., Rectangular Filament-Wound Glass Fibre Reinforced Polymer Tubes Filled with Concrete under Flexural and Axial Loading: Experimental Investigation. *Journal of Composites for Construction,* **9(1)**, 25-33 (2005).
2. Fam, A., and Skutezky, T., Composite T-Beams Using Reduced-Scale Rectangular FRP Tubes and Concrete Slabs. *Journal of Composites for Construction,* **10(2)**, 172-181 (2006).
3. Gai, X., Darby, A.P., Ibell, T.J., and Evernden, M.C., Permanent Participating FRP Formwork for Concrete Floor Slabs presented at the *10th International Research Symposium on Fibre Reinforced Concrete Structures,* Tampa, April 2-4, 2011.